

# A consistent dynamic localization model for large eddy simulation based on a variational formulation

By V. Gravemeier<sup>†</sup>

## 1. Motivation and objectives

The modeling of the unresolved or subgrid scales is a crucial aspect of large eddy simulation (LES) of turbulent flows. A very popular method of modeling relies on the subgrid (or eddy) viscosity concept, which is based on the Boussinesq turbulent (or eddy) viscosity assumption. According to this concept, the deviatoric part of the subgrid-scale stress tensor  $\tau$  is approximated by a product of a subgrid viscosity  $\nu_T$  and the rate-of-strain tensor of the resolved scales. The remaining unknown in this modeling approach is the subgrid viscosity  $\nu_T$ . Several approximations for  $\nu_T$  have been proposed. The Smagorinsky model was the earliest approach in this context and is still commonly used due to its simplicity. However, that model is based on an unknown parameter  $C_S$ . Choosing a constant value for this parameter over the entire domain has been proven to be an inadequate approach in most of the cases, although recent integrations of this simple constant-coefficient-based Smagorinsky model into a multiscale environment have revitalized it and have yielded very good results for a number of test cases (see, for example, Gravemeier (2005b) and references therein). An important improvement of the Smagorinsky model was introduced in Germano *et al.* (1991), in which the model parameter was determined as a function of position and time by way of a dynamic algorithm. It should be remarked that this dynamic procedure is not restricted to the Smagorinsky model as the underlying model, although it has mostly been used with that model.

The original formulation of the dynamic algorithm in Germano *et al.* (1991) contains a mathematically inconsistent assumption that disregards the fact that  $C_S$  is a rapidly varying function of position, as discussed in Moin (1991). This inconsistency was later overcome in Ghosal *et al.* (1995) by the introduction of the dynamic localization model. Furthermore, *ad hoc* schemes were proposed in that publication, which were usually applied in practical simulations to prevent them from becoming unstable. By using those *ad hoc* schemes, the application of the dynamic model in several problem configurations was enabled, though without being justified except in a heuristic way. Overall, the study by Ghosal *et al.* (1995) aimed at “putting the dynamic modeling procedure on firm theoretical foundations, so that the method could be applied to arbitrary inhomogeneous flows without recourse to *ad hoc* procedures”. After all, however, the actual method of calculating the model parameter based on a variationally formulated condition for  $C_S$ , which eventually had to make use of Fredholm’s integral equation of the second kind for its solution, appeared to be rather complicated. Moreover, an iterative procedure was necessary to solve this integral equation in practical calculations, which made it a computationally expensive part of the overall simulation.

<sup>†</sup> Current address: Technical University of Munich, Chair for Computational Mechanics, Boltzmannstr. 15, D-85747 Garching, Germany. E-mail: vgravem@lnm.mw.tum.de

In the present study, LES is based on a variational formulation. In contrast to a traditional filter-based formulation, the resolution of the underlying numerical discretization is used to define the resolved part of the velocity  $\mathbf{u}^h$ , with the superscript  $h$  indicating the characteristic length scale of the discretization. It should be remarked that this is actually a usual way of defining the resolved scales in practical LES whenever the respective discretization is assumed to act as an implicit filter, and no further explicit filter is applied. The reason for introducing a subgrid-scale model in the variational formulation is mathematically different from the usual necessity of introducing a model term due to the appearance of a subgrid-scale stress tensor in the strong formulation of the Navier-Stokes equations in a traditional LES. Nevertheless, the physical necessity of accounting for the missing effect of unresolved scales on the resolved scales is the same in both cases. In order to account for this effect in the present study, the present study uses both the subgrid viscosity concept and the Smagorinsky model as the particular approach to modeling the unresolved scales. Within a variational formulation of the Navier-Stokes equations, the variationally formulated condition for  $C_S$  in the dynamic localization model according to Ghosal *et al.* (1995) may easily be integrated to acquire a system of two variational equations. Hence, a consistent formulation is achieved; both the underlying equation system (i.e. the incompressible Navier-Stokes equations) and the equation for  $C_S$  are in variational form.

A crucial ingredient of a dynamic modeling procedure is the separation of the resolved scales into large and small resolved scales. While this separation may easily be done in spectral space by using a sharp cut-off filter, discrete smooth filters are usually applied in physical space. However, scale-separating operators based on combined multigrid operators were recently proposed in Gravemeier (2005a) as an alternative way of separating the scales. A similar multigrid approach within a finite volume method was proposed in Terracol *et al.* (2001). It was shown in Gravemeier (2005a) that multigrid-based scale-separating operators, in particular those that provide a projective scale separation, are superior to discrete smooth filters in terms both of quality of results and of computational efficiency. This projective operator also serves as the basis for the version of the dynamic localization model to be developed in this work. The final variational equation system may serve as the starting point for either a finite element or a finite volume formulation. In this work, all theoretical developments will be presented in a general manner, so that both finite element and finite volume implementations may easily be derived from it. The simulations at the end of this study have been conducted using the CDP- $\alpha$  code (Mahesh *et al.* 2004), the flagship LES code of the Center for Turbulence Research. Underlying this code is a finite volume method particularly suited for applications in complex geometries on unstructured grids. The consistent dynamic localization model developed in the present work is applied to turbulent flow in a channel. A detailed version of the present study can be found in Gravemeier (2005c) containing, among other things, the application of the proposed dynamic localization model to turbulent flow in a planar asymmetric diffuser.

## 2. Variational formulation and separation of scales

A variational form of the Navier-Stokes equations may be achieved by starting with a weighted residual formulation:

$$B_{\text{NS}}(\mathbf{v}, q; \mathbf{u}, p) = (\mathbf{v}, \mathbf{f})_{\Omega} \quad \forall \{\mathbf{v}, q\} \in \mathcal{V}_{\mathbf{u}p}, \quad (2.1)$$

where  $\mathbf{v}$  and  $q$  denote the weighting functions, and  $\mathcal{V}_{\mathbf{u}p}$  denotes the combined form of the weighting function spaces for velocity and pressure in the sense that  $\mathcal{V}_{\mathbf{u}p} := \mathcal{V}_{\mathbf{u}} \times \mathcal{V}_p$ . The form  $B_{\text{NS}}(\mathbf{v}, q; \mathbf{u}, p)$  on the left hand side is hereby defined as

$$B_{\text{NS}}(\mathbf{v}, q; \mathbf{u}, p) = \left( \mathbf{v}, \frac{\partial \mathbf{u}}{\partial t} \right)_{\Omega} + (\mathbf{v}, \nabla \cdot (\mathbf{u} \otimes \mathbf{u}))_{\Omega} + (\mathbf{v}, \nabla p)_{\Omega} - (\mathbf{v}, \nabla \cdot (2\nu \varepsilon(\mathbf{u})))_{\Omega} + (q, \nabla \cdot \mathbf{u})_{\Omega}. \quad (2.2)$$

The weighted residual formulation defined in (2.1)-(2.2) may serve as the starting point for either a finite element or a finite volume formulation. A detailed discussion of these two formulations can be found in Gravemeier (2005b).

In either case, the prerequisite for the application of the respective method is a discretization of the domain  $\Omega$  into  $n$  elements or control volumes  $\Omega_i$  ( $i = 1, \dots, n$ ) with element or control volume boundaries  $\Gamma_i$ , respectively. In the following, it will be referred to  $\Omega_i$  as an “element” for brevity, which is, however, assumed to be replaced by the notation “control volume” in the context of the finite volume method. With  $h$  denoting the characteristic length scale of the discretization, the variational formulation for the discrete weighting and solution functions reads as

$$B_{\text{NS}}(\mathbf{v}^h, q^h; \mathbf{u}^h, p^h) = (\mathbf{v}^h, \mathbf{f})_{\Omega} \quad \forall \{\mathbf{v}^h, q^h\} \in \mathcal{V}_{\mathbf{u}p}^h, \quad (2.3)$$

where  $\mathcal{V}_{\mathbf{u}p}^h$  indicates the discrete weighting function space, and the appropriate integration-by-parts procedures have to be implemented for either the finite element or the finite volume method, see Gravemeier (2005b). In LES, the characteristic length scale  $h$  is usually considerably larger than the order of the smallest length scale of the problem. Thus, a large number of scales cannot be explicitly resolved. Therefore, the subgrid viscosity approach is applied in order to take into account the (dissipative) effect of the unresolved scales. According to this, a subgrid viscosity term in weighted formulation is added to (2.3), resulting in

$$B_{\text{NS}}(\mathbf{v}^h, q^h; \mathbf{u}^h, p^h) - (\mathbf{v}^h, \nabla \cdot (2\nu_{\text{T}} \varepsilon(\mathbf{u}^h)))_{\Omega} = (\mathbf{v}^h, \mathbf{f})_{\Omega} \quad \forall \{\mathbf{v}^h, q^h\} \in \mathcal{V}_{\mathbf{u}p}^h, \quad (2.4)$$

where  $\nu_{\text{T}}$  denotes the subgrid viscosity. The weighted subgrid viscosity term in (2.4) is also given without any integration-by-parts procedure. This is in order to keep the notation open for the application of the respective numerical method, which eventually results in a variationally formulated subgrid viscosity term. The goal of this work is to find appropriate modeling approaches for the subgrid viscosity  $\nu_{\text{T}}$  in the context of a variational formulation. Before turning to this issue, effective ways to separate the resolved scales of the problem, that is, to differentiate the larger and the smaller resolved scales, are required.

The scale separation used in this work relies on combined multigrid operators, originally presented in Gravemeier (2005a). It refers to the level of complete resolution indicated by the characteristic length  $h$  and identifies *a priori* a large-scale resolution level with respect to this complete resolution level characterized by the length  $\bar{h}$ , where  $\bar{h} > h$ . As a result, a large-scale part of the velocity  $\bar{\mathbf{u}}^h$  on the large-scale resolution level is extracted. The small-scale part of the velocity is consistently defined on the level of complete resolution, which is characterized by the length  $h$ , as

$$\mathbf{u}^h = \mathbf{u}^h - \bar{\mathbf{u}}^h, \quad (2.5)$$

where  $\bar{\mathbf{u}}^h$  is the large-scale value transferred to this level. In practice, two grids are created: a coarser grid, which is called the “parent” grid, and a finer grid, which is called the

“child” grid. The child grid is obtained by an isotropic hierarchical subdivision of the parent grid. More details concerning the implementation can be found in Gravemeier (2005a).

The general class of scale-separating operators based on multigrid operators is formulated as

$$\bar{\mathbf{u}}^h = S^m [\mathbf{u}^h] = P \circ R [\mathbf{u}^h] = P [\bar{\mathbf{u}}^h], \quad (2.6)$$

where the scale-separating operator  $S^m$  consists of the sequential application of a restriction operator  $R$  and a prolongation operator  $P$ . Applying the restriction operator on  $\mathbf{u}^h$  yields a large-scale velocity  $\bar{\mathbf{u}}^h$  defined at the degrees of freedom of the parent grid, which is then prolonged, in order to obtain a large-scale velocity  $\bar{\mathbf{u}}^h$  defined at the degrees of freedom of the child grid. Various restriction as well as prolongation operators may be used in (2.6). Two special combinations of restriction and prolongation operators were analyzed and used in Gravemeier (2005a). Both rely on the same restriction operator but apply different prolongation operators afterwards. The restriction operator  $R$  is defined as a volume-weighted average over all the child elements within one parent element subject to

$$\bar{\mathbf{u}}_j^h = \frac{\sum_{i=1}^{n_{\text{cop}}} |\Omega_i| \mathbf{u}_i^h}{\sum_{i=1}^{n_{\text{cop}}} |\Omega_i|}, \quad (2.7)$$

where  $\bar{\mathbf{u}}_j^h$  denotes the large-scale velocity at the center of the parent element  $\bar{\Omega}_j$  and  $n_{\text{cop}}$  the number of child elements in  $\bar{\Omega}_j$ . The prolongation operator  $P^p$  used in this work yields a constant prolongation as

$$\bar{\mathbf{u}}_i^h = P^p [\bar{\mathbf{u}}_j^h]_i = \bar{\mathbf{u}}_j^h \quad \forall \Omega_i \subset \bar{\Omega}_j \quad (2.8)$$

and zero elsewhere. The complete scale-separating operator is defined as  $S^{\text{pm}} := P^p \circ R$ . The property of a projector is indicated by the additional superscript “p”.

### 3. Consistent dynamic localization model

The dynamic modeling procedure to be presented below uses the Smagorinsky model as its underlying model formulation. Thus, the subgrid viscosity is given as

$$\nu_{\text{T}} = (C_S h)^2 |\varepsilon(\mathbf{u}^h)|, \quad (3.1)$$

where  $\varepsilon(\mathbf{u}^h)$  denotes the rate-of-strain tensor of the resolved scales. It was originally proposed in Germano *et al.* (1991) and relies on the Germano identity. This identity refers to a point-wise formulation of the Navier-Stokes equations for the discretized variables  $\mathbf{u}^h$  and  $p^h$ , which already contains a subgrid-scale stress tensor to account for the scales still unresolved by this discretization. This subgrid-scale stress tensor can be defined as

$$\boldsymbol{\tau}^h = (\mathbf{u} \otimes \mathbf{u})^h - \mathbf{u}^h \otimes \mathbf{u}^h. \quad (3.2)$$

Note that in (3.2) the usual filtered formulation is replaced by the actual implicit scale separation based on the chosen discretization with characteristic length scale  $h$ . The “test filter” is replaced by the scale-separating operator  $S^{\text{pm}}$ . Thus, the analog of the

“subtest”-scale stress tensor can be expressed as

$$\bar{\boldsymbol{\tau}}^h = S^{\text{pm}} \left[ (\mathbf{u} \otimes \mathbf{u})^h \right] - S^{\text{pm}} \left[ \mathbf{u}^h \right] \otimes S^{\text{pm}} \left[ \mathbf{u}^h \right] \quad (3.3)$$

The Germaino identity states the following:

$$\mathbf{L}^h = \bar{\boldsymbol{\tau}}^h - S^{\text{pm}} \left[ \boldsymbol{\tau}^h \right], \quad (3.4)$$

where  $\mathbf{L}^h$  can be obtained as

$$\mathbf{L}^h = S^{\text{pm}} \left[ \mathbf{u}^h \otimes \mathbf{u}^h \right] - S^{\text{pm}} \left[ \mathbf{u}^h \right] \otimes S^{\text{pm}} \left[ \mathbf{u}^h \right] \quad (3.5)$$

by inserting (3.2) and (3.3) into (3.4).

Assuming the Smagorinsky model as an appropriate modeling term at both discretization levels, and accounting for the fact that the Smagorinsky model is basically a “trace-free” model in the context of incompressible flow, equation (3.4) is modeled as follows:

$$\begin{aligned} \text{dev} \mathbf{L}^h &= \mathbf{L}^h - \frac{1}{3} \text{tr} \mathbf{L}^h \mathbf{I} \\ &\approx -2 (C_S \bar{h})^2 \left| S^{\text{pm}} \left[ \boldsymbol{\varepsilon}(\mathbf{u}^h) \right] \right| S^{\text{pm}} \left[ \boldsymbol{\varepsilon}(\mathbf{u}^h) \right] + S^{\text{pm}} \left[ 2 (C_S h)^2 \left| \boldsymbol{\varepsilon}(\mathbf{u}^h) \right| \boldsymbol{\varepsilon}(\mathbf{u}^h) \right] \end{aligned} \quad (3.6)$$

where  $\mathbf{I}$  denotes the identity tensor and modeling is obviously confined to the deviatoric part of the tensor  $\mathbf{L}^h$ . According to a usual implementation of the dynamic modeling procedure, it would now be assumed that  $C_S$  is constant over one element of the parent grid. Hence, equation (3.6) may be rewritten as

$$\text{dev} \mathbf{L}^h \approx C_S^h \left( 2 S^{\text{pm}} \left[ \left| \boldsymbol{\varepsilon}(\mathbf{u}^h) \right| \boldsymbol{\varepsilon}(\mathbf{u}^h) \right] - 2 \left( \frac{\bar{h}}{h} \right)^2 \left| S^{\text{pm}} \left[ \boldsymbol{\varepsilon}(\mathbf{u}^h) \right] \right| S^{\text{pm}} \left[ \boldsymbol{\varepsilon}(\mathbf{u}^h) \right] \right), \quad (3.7)$$

where the parameter expression  $(C_S h)^2$  is denoted by  $C_S^h$  here and below. This assumption neglects the important observation that  $C_S$  is a rapidly varying function of position, see Moin (1991). This observation gave rise to the development of the dynamic localization model in Ghosal *et al.* (1995). In that model, the parameter expression  $C_S^h$  is not taken out of the scale-separating operation and the related mathematical inconsistency is therefore taken back. As a result, the error tensor with respect to the approximate fulfillment of (3.6) may be written as

$$\mathbf{E}^h = \text{dev} \mathbf{L}^h - C_S^h \mathbf{A}^h + S^{\text{pm}} \left[ C_S^h \mathbf{B}^h \right], \quad (3.8)$$

where

$$\mathbf{A}^h = -2 \left( \frac{\bar{h}}{h} \right)^2 \left| S^{\text{pm}} \left[ \boldsymbol{\varepsilon}(\mathbf{u}^h) \right] \right| S^{\text{pm}} \left[ \boldsymbol{\varepsilon}(\mathbf{u}^h) \right], \quad (3.9)$$

and

$$\mathbf{B}^h = -2 \left| \boldsymbol{\varepsilon}(\mathbf{u}^h) \right| \boldsymbol{\varepsilon}(\mathbf{u}^h). \quad (3.10)$$

The scale-separating operator  $S^{\text{pm}}$  in (3.8) raises the dependency of the value for  $C_S^h$  in one child element to all other child elements within the same parent element. Due to the extended dependency, a minimization procedure restricted to one point, as in a typical dynamic modeling procedure, is no longer possible. Thus, the functional

$$\mathcal{F} \left[ C_S^h \right] = \int_{\Omega} \mathbf{E}^h \mathbf{E}^h \, d\Omega \quad (3.11)$$

was chosen in Ghosal *et al.* (1995) to enforce a minimization in an integral sense over

the entire domain  $\Omega$ . Setting the variation of  $\mathcal{F}$  to zero results in

$$\delta\mathcal{F} [C_S^h] = 2 \int_{\Omega} \delta\mathbf{E}^h \mathbf{E}^h d\Omega = 0. \quad (3.12)$$

In Ghosal *et al.* (1995), a strong solution of the corresponding Euler-Lagrange equation was sought. This led to a complicated equation for  $C_S^h$  in the format of Fredholm's integral equation of the second kind, which was solved in an iterative procedure. All of this is not necessary here. Instead, this work proposes that equation (3.12) be considered as another variational equation to be solved in addition to the basic variational equation (2.4). Thus, a system of two variational equations is established.

The solution of (3.12) may follow the so-called "variational principle", a concept well-known in the context of the finite element method. Consult a standard textbook on the finite element method for elaboration. The variational principle specifies a functional depending in an integral form on an unknown function, which is here represented by the functional  $\mathcal{F}$  and by the unknown function  $C_S^h(\mathbf{x}, t)$ . The solution to the problem is a function  $C_S^h$  which makes  $\mathcal{F}$  stationary with respect to small changes  $\delta C_S^h$ . For this purpose, the variation  $\delta\mathcal{F}$  is set to zero, as shown in (3.12). The small change  $\delta C_S^h$  is implicitly contained in the small change  $\delta\mathbf{E}^h$  in the error tensor function  $\mathbf{E}^h$  in (3.12) and will be revealed below. As aforementioned, the variational principle is well-established in the finite element method, but only for problems, for which such a functional can be found. This requirement excludes a multitude of mechanical problems, including the present Navier-Stokes problem. Thus, the Navier-Stokes equations have been introduced into a weighted residual formulation above, which is the alternative and more general concept within the finite element method. However, both concepts - the weighted residual formulation and the variational principle - eventually lead to a variational formulation in the finite element method.

The problem is that in general, the variational principle is not an appropriate concept in the finite volume method, as the latter is intended to be applied in the numerical simulations below. However, under the particular circumstances of this relatively simple case (i.e. no derivatives of  $C_S^h$  are contained in the error tensor function (3.8)), a similar solution approach for (3.12) may also be pursued with the finite volume method. Inserting (3.8) into (3.12) yields

$$2 \int_{\Omega} (-\delta C_S^h \mathbf{A}^h + S^{\text{pm}} [\delta C_S^h \mathbf{B}^h]) (\text{dev} \mathbf{L}^h - C_S^h \mathbf{A}^h + S^{\text{pm}} [C_S^h \mathbf{B}^h]) d\Omega = 0, \quad (3.13)$$

which can be rearranged as

$$\begin{aligned} & \int_{\Omega} \delta C_S^h \mathbf{A}^h C_S^h \mathbf{A}^h d\Omega - \int_{\Omega} \delta C_S^h \mathbf{A}^h S^{\text{pm}} [C_S^h \mathbf{B}^h] d\Omega \\ & - \int_{\Omega} S^{\text{pm}} [\delta C_S^h \mathbf{B}^h] C_S^h \mathbf{A}^h d\Omega + \int_{\Omega} S^{\text{pm}} [\delta C_S^h \mathbf{B}^h] S^{\text{pm}} [C_S^h \mathbf{B}^h] d\Omega \\ & = \int_{\Omega} \delta C_S^h \mathbf{A}^h \text{dev} \mathbf{L}^h d\Omega - \int_{\Omega} S^{\text{pm}} [\delta C_S^h \mathbf{B}^h] \text{dev} \mathbf{L}^h d\Omega \end{aligned} \quad (3.14)$$

The first line of (3.14) contains the terms including the non-projected weighting function  $\delta C_S^h$ , the second line the terms including the projected weighting function  $\delta C_S^h$ , and the third line the known terms depending on the deviatoric part of the tensor  $\mathbf{L}^h$ , weighted either by the non-projected or by the projected weighting function  $\delta C_S^h$ .

Note that (3.14) does not contain any derivatives of the function  $C_S^h$ . Thus, a third

crucial advantage of the present approach with respect to Ghosal *et al.* (1995), aside from the advantages of a simpler formulation and the eliminated need for an iterative solution approach, can be attributed to the fact that (3.14) does not need to be solved as a global equation over the entire domain. Rather, it may be solved as a number of substantially smaller local equations, since the coupling of the values due to  $S^{\text{pm}}$  exists only within the range of each parent element. Thus, a sample equation defined in the parent element  $\bar{\Omega}_j$  is given as

$$\begin{aligned}
 & \sum_{i=1}^{n_{\text{cop}}} \int_{\Omega_i} \delta C_S^h \mathbf{A}^h C_S^h \mathbf{A}^h d\Omega - \sum_{i=1}^{n_{\text{cop}}} \int_{\Omega_i} \delta C_S^h \mathbf{A}^h S^{\text{pm}} [C_S^h \mathbf{B}^h] d\Omega \\
 & - \sum_{i=1}^{n_{\text{cop}}} \int_{\Omega_i} S^{\text{pm}} [\delta C_S^h \mathbf{B}^h] C_S^h \mathbf{A}^h d\Omega + \sum_{i=1}^{n_{\text{cop}}} \int_{\Omega_i} S^{\text{pm}} [\delta C_S^h \mathbf{B}^h] S^{\text{pm}} [C_S^h \mathbf{B}^h] d\Omega \\
 & = \sum_{i=1}^{n_{\text{cop}}} \int_{\Omega_i} \delta C_S^h \mathbf{A}^h \text{dev} \mathbf{L}^h d\Omega - \sum_{i=1}^{n_{\text{cop}}} \int_{\Omega_i} S^{\text{pm}} [\delta C_S^h \mathbf{B}^h] \text{dev} \mathbf{L}^h d\Omega \quad (3.15)
 \end{aligned}$$

where, again,  $n_{\text{cop}}$  denotes the number of child elements  $\Omega_i$  in  $\bar{\Omega}_j$ . All equations of type (3.15) can be solved independently. Thus, they are parallel to full extent in a multi-processor calculation, resulting in substantial computational savings.

Only volume integrals need be dealt with in equation (3.14). These may likewise be defined over element domains in a finite element method, or over control volume domains in a finite volume method. The simplest approximation is chosen here by using discontinuous ansatz functions for the weighting and solution functions in a finite element method as well as for the solution function in a finite volume method. The weighting function in a finite volume method is already defined to be constant *a priori* (i.e.  $\delta C_S^h = 1$  for the present case). In the end, one equation of type (3.15) has to be solved in each parent element. Thus, the overall number of equations that have to be solved equals the number of parent elements in the domain. The matrices resulting from each of these equations are of size  $n_{\text{cop}} \times n_{\text{cop}}$ . Usually (i.e. for hexahedral and tetrahedral elements), these amount to  $8 \times 8$  matrices. In the numerical simulations below, a direct solver, which is contained in the LAPACK solver package for dense linear systems, is used for the solution of these relatively small matrices.

Although the mathematical inconsistency is adequately addressed by this approach, the problem of obtaining potentially negative values for  $C_S^h$  and, hence, for  $C_S$  still exists. In Ghosal *et al.* (1995), the constraint  $C_S \geq 0$  was directly imposed. Analogous to this, clipping in the sense that  $C_S^h = (1/2) (C_S^h + |C_S^h|)$  is also enforced for the numerical simulations of this work. Thus, the present approach resembles the dynamic localization model (constrained) in Ghosal *et al.* (1995).

An alternative model, which is called the dynamic localization model ( $k$ -equation), was also proposed in Ghosal *et al.* (1995). The crucial feature of this model is that it allows for backscatter of energy (i.e.  $C_S$  is allowed to take negative values). The subgrid-scale kinetic energy  $k$  is monitored, though, in order to rule out unphysical negative values. The drawback of this model is the enormous effort linked with it. Since the subgrid-scale kinetic energy appears in the model formulation, a global transport equation must be solved for  $k$ . The present approach is basically open to this. In this case, the already existing system of two variational equations would be extended by an additional global scalar equation, which also might be solved as a variational equation. Furthermore, two equations would have to be solved for two parameters appearing in the transport equation

for  $k$ . These equations are similar in their structure to the one that has to be solved for  $C_S^h$  (i.e. they may also be dealt with as a number of local equations). Thus, the dynamic localization model ( $k$ -equation) in the context of the present approach would require the solution of one additional global equation and of two additional local equation systems.

#### 4. Numerical results

The numerical setup for turbulent flow in a channel is basically identical to the one described in Gravemeier (2005a). Flows at two different Reynolds numbers,  $Re_\tau = u_\tau \delta_c / \nu = 180$  and  $Re_\tau = 590$ , are simulated marking the lower and upper end of the DNS study in Moser *et al.* (1999).  $u_\tau$  and  $\delta_c$  denote the turbulent wall-shear velocity and the channel half-width, respectively. In the first part of the channel flow study, the flow at the lower Reynolds number is investigated, with a spatial discretization using 32 control volumes in each coordinate direction. In the second part, a grid refinement study for the flow at the higher Reynolds number is conducted using the grid with 32 control volumes in each coordinate direction for this case as well. Furthermore, grids employing 48, 64, and 80 control volumes, respectively, are applied. The usual dynamic model with averaging and clipping will be abbreviated “DAMC” (Dynamic Averaged Model with Clipping), and the proposed dynamic localization model (constrained) will be abbreviated “DLMC” below.

At first, the mean streamwise resolved velocity is analyzed for the flow at  $Re_\tau = 180$  in Fig. 1. Due to the second-order accuracy of the underlying numerical method and to the relatively coarse discretization, all LES profiles depart considerably from the DNS profile. The differences between DAMC and DLMC are relatively small in both cases. It is emphasized that none of the dynamic modeling approaches provide better results than the ones obtained with no model (NM). This is in accordance with results in Kravchenko & Moin (1997) and in Shah & Ferziger (1995), where a second-order accurate numerical method was used for simulations with DAMC and, among other things, compared to no-model calculations. For the mean streamwise velocity profiles, DAMC was more or less clearly outperformed by NM at even higher Reynolds numbers ( $Re_\tau = 1000$  and  $Re_\tau = 1800$ ) than were the ones investigated in the present study. Notable deviations of the profiles from the respective DNS profiles due to the use of a second-order accurate method, combined with a relatively coarse resolution, were also observed in Terracol *et al.* (2001) for flows at the same Reynolds numbers used in the present work. All those observations, including the ones made in this study, raise general doubts about the usefulness of any dynamic subgrid-scale modeling approach of this form within a second-order accurate numerical method.

The turbulent kinetic energy of the resolved scales is investigated in Fig. 2. As for the mean streamwise resolved velocity, little difference between any of the applied methods can be recognized. The only notable discrepancy is produced by DAMC for the peak of the turbulent kinetic energy. This peak is considerably more over-predicted by this method. The mean value of the dynamically determined model parameter  $C_S$  is evaluated and compared in Fig. 3. The profiles for both methods are similar. Slightly higher values are obtained for DLMC in comparison to DAMC. In Fig. 4, the profiles for the root-mean-square value  $C_S^{\text{rms}}$  of the dynamically determined parameter  $C_S$  are shown. Significant discrepancies between DAMC and DLMC can be observed. With  $C_S^{\text{rms}}$  almost negligible for DAMC, very high values, including distinct peaks, are obtained with DLMC. This confirms that a rapidly varying function  $C_S$  is indeed produced by the

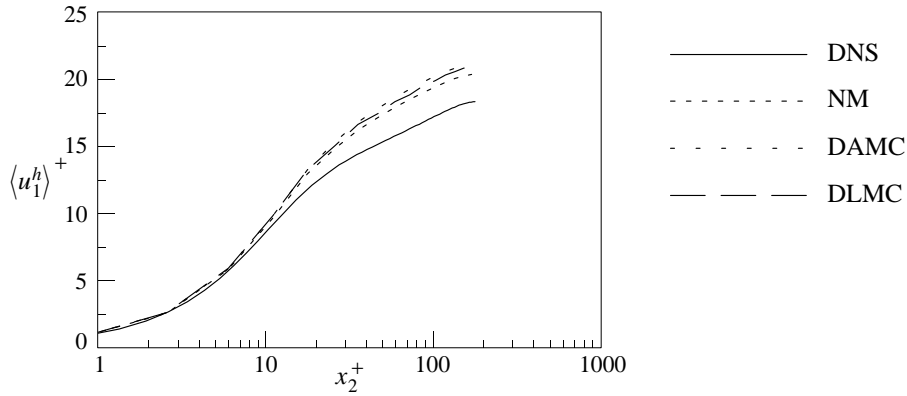


FIGURE 1. Mean streamwise velocity at  $Re_\tau = 180$

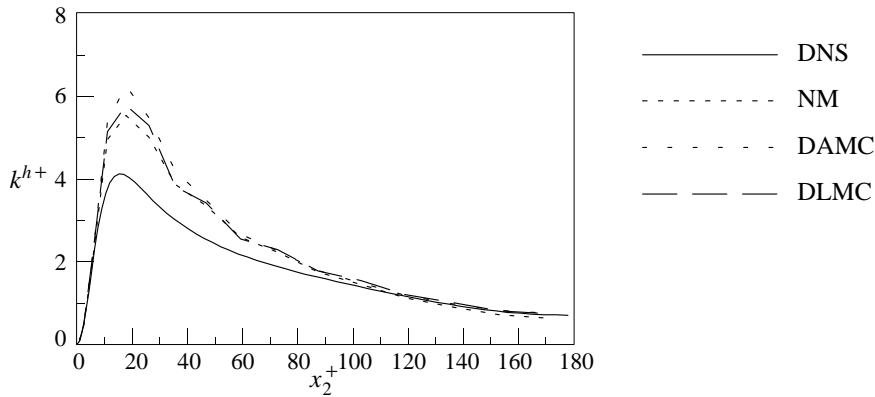
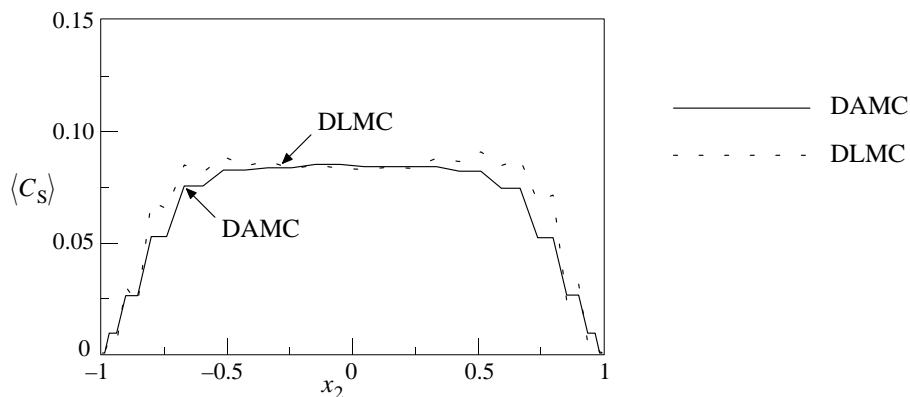
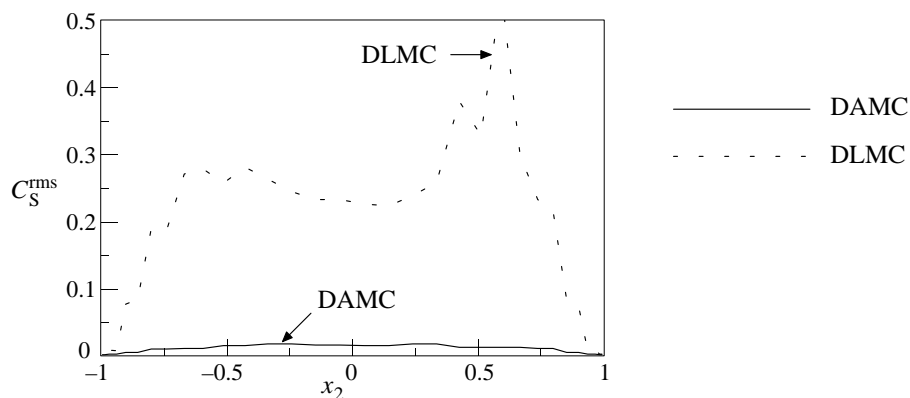


FIGURE 2. Turbulent kinetic energy at  $Re_\tau = 180$

dynamic localization model, which is consistent with the original intention for introducing this model in Ghosal *et al.* (1995). The picture can be quantified by determining volume-averaged mean and root-mean-square values for  $C_S$  over the entire domain. The mean values are very close for both methods, as already observable in Fig. 3. However, substantially higher root-mean-square values are yielded by DLMC than by DAMC. The root-mean-square value is about 15% of the mean value for DAMC. For DLMC, this ratio exceeds 300% (i.e. the standard deviation amounts to more than three times the mean value).

In the second part of the channel flow study, the influence of the discretization level is investigated for the flow at the higher Reynolds number. Figure 5 shows the mean streamwise resolved velocity for this case using four different discretization levels. By comparing Figs. 5(a) and 5(b), it is observed that both DAMC and DLMC yield approximately the same convergence to the DNS profile for the two coarser discretizations. However, for the two finer discretizations, and in particular for the one with 80 control volumes in each coordinate direction, DAMC provides a prediction of the velocity profile that is notably closer to the DNS profile than does the one for DLMC. The grid refinement effect on the mean value and the root-mean-square value of the model parameter  $C_S$  is also analyzed. The quantitative results are provided in the tables displayed as Figs. 6 and 7, respectively. The mean values, the root-mean-values, as well as the ratio of these two

FIGURE 3. Mean value of model parameter  $C_S$  at  $Re_\tau = 180$ FIGURE 4. Root-mean-square value of model parameter  $C_S$  at  $Re_\tau = 180$ 

values, are decreasing for both methods with one exception when the discretization level increases. In column (4) of both tables, the statistics of the clipping procedure (i.e. the *ad hoc* measure common to both methods) are given. It is obvious that after averaging in the case of DAMC, few control volumes have to be clipped. This clipping percentage ranges from about 12.5% of all control volumes for the coarsest discretization, to no clipping at all for the finest discretization. For DLMC, there is substantial need for clipping. Between 45% and 48% of all control volumes are clipped in the investigated cases, with only a slight decrease for the finer discretizations.

## 5. Conclusions

A new approach for a dynamic localization model has been proposed in this work. This approach has been consistently integrated into LES based on a variational formulation, since the variationally formulated condition for the model parameter has been considered as an additional equation in a resulting system of two variational equations. This variational system may be solved using either a finite element or a finite volume method. The new version of the dynamic localization proposed in this work has three important advantages compared to the original dynamic localization model in Ghosal *et al.* (1995).

- The solution of the new dynamic localization model is based on a simpler formu-

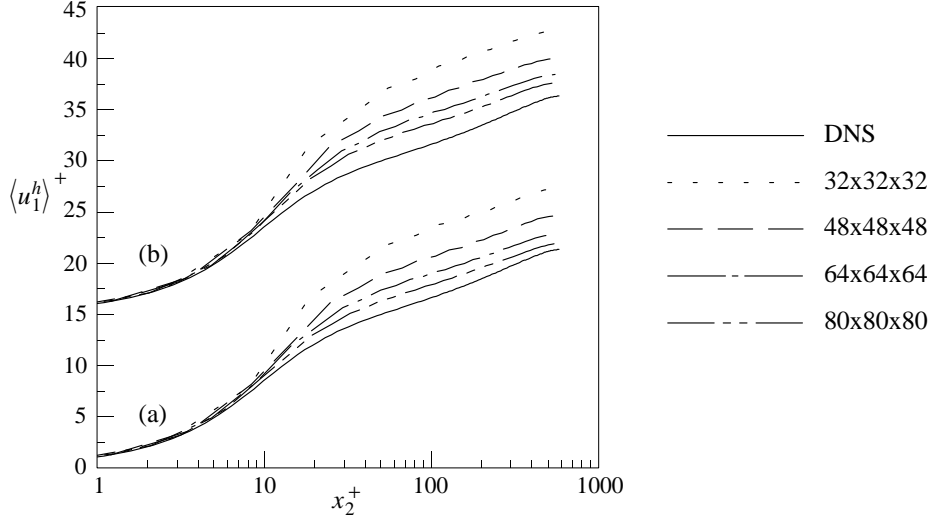


FIGURE 5. Grid refinement effect on mean streamwise velocity at  $Re_\tau = 590$ : (a) DAMC; (b) DLMC (+15)

	(1): mean value	(2): rms value	(3)=(2)/(1) [%]	(4): clipped cv [%]
32x32x32	0.078	0.009	11.12	12.49
48x48x48	0.075	0.006	7.67	7.59
64x64x64	0.073	0.004	5.64	2.06
80x80x80	0.066	0.003	4.92	0.00

FIGURE 6. Volume-averaged mean and root-mean-square values of model parameter  $C_S$  and clipping percentage at  $Re_\tau = 590$ : DAMC on various discretizations

	(1): mean value	(2): rms value	(3)=(2)/(1) [%]	(4): clipped cv [%]
32x32x32	0.086	0.342	398.02	47.70
48x48x48	0.081	0.259	319.49	46.89
64x64x64	0.077	0.272	352.90	45.93
80x80x80	0.068	0.231	341.46	44.92

FIGURE 7. Volume-averaged mean and root-mean-square values of model parameter  $C_S$  and clipping percentage at  $Re_\tau = 590$ : DLMC on various discretizations

lation, since the variationally formulated condition for the model parameter is actually solved as a variational equation. This obviates the need to use a complicated Fredholm integral equation of the second kind for its solution, as in Ghosal *et al.* (1995).

- The solution of the integral equation as proposed in Ghosal *et al.* (1995) had to be done iteratively. This is not necessary for the new approach, since it may simply be solved as a linear variational equation.

- A number of small independent local equations equal to the number of parent elements or control volumes can be solved instead of solving one large global equation as in Ghosal *et al.* (1995). Thus, the actual solution procedure may be executed completely in parallel in a multi-processor simulation, in contrast to required inter-processor communications during the solution of a global equation.

Moreover, it should be emphasized that no approximation (in time), as in Piomelli & Liu (1995), and no exploitation of any homogeneous flow directions, as in Wang *et al.* (2004), have been necessary in the development of this new approach. The *ad hoc* measure remaining in the present approach is a clipping procedure for elements or control volumes exhibiting negative values of  $C_S$ . The clipping is done to prevent potential instabilities in the course of the simulation. However, a similar measure had to be taken for the dynamic localization model (constrained) in Ghosal *et al.* (1995). A few hints for a potential extension of the consistent dynamic localization model (constrained) to a consistent dynamic localization model ( $k$ -equation) based on the one proposed in Ghosal *et al.* (1995) have been given at the end of section 3.

### Acknowledgments

The partial support by the Alexander von Humboldt-Foundation through a Feodor Lynen Fellowship is gratefully acknowledged. The author would also like to thank Parviz Moin and Gregory Burton for helpful discussions.

### REFERENCES

- GERMANO, M., PIOMELLI, U., MOIN, P. & CABOT, W. H. 1991 A dynamic subgrid-scale eddy viscosity model. *Phys. Fluids* **3**, 1760-1765.
- GHOSAL, S., LUND, T. S., MOIN, P. & AKSELVOLL, K. 1995 A dynamic localization model for large-eddy simulation of turbulent flows. *J. Fluid Mech.* **286**, 229-255.
- GRAVEMEIER, V. 2005a Scale-separating operators for variational multiscale large eddy simulation of turbulent flows. *J. Comp. Phys.*, **212**, 400-435.
- GRAVEMEIER, V. 2005b The variational multiscale method for laminar and turbulent flow. *Arch. Comp. Meth. Engrg.*, in press.
- GRAVEMEIER, V. 2005c A consistent dynamic localization model for large eddy simulation of turbulent flows based on a variational formulation. *Preprint*, submitted for publication in *J. Comp. Phys.*.
- KRAVCHENKO, A. G. & MOIN, P. 1997 On the effect of numerical errors in large eddy simulations of turbulent flows. *J. Comp. Phys.* **131**, 310-322.
- MAHESH, K., CONSTANTINESCU, G. & MOIN, P. 2004 A numerical method for large eddy simulation in complex geometries. *J. Comp. Phys.* **197**, 215-240.
- MOIN, P. 1991 A dynamic localization model for large-eddy simulation of turbulent flows. In: *Proc. Monte Verita Coll. on Turbulence*, Birkhaeuser, Bale.
- MOSER, R. D., KIM, J. & MANSOUR, N. N. 1999 Direct numerical simulation of turbulent channel flow up to  $Re_\tau = 590$ . *Phys. Fluids* **11**, 943-945.
- PIOMELLI, U. & LIU, J. 1995 Large eddy simulation of rotating channel flows using a localized dynamic model. *Phys. Fluids* **7**, 839-848.
- SHAH, K. B. & FERZIGER, J. H. 1995 A new non-eddy viscosity subgrid-scale model and its application to channel flow. *Annual Research Briefs - 1995*, Center for Turbulence Research, NASA Ames/Stanford Univ., 73-90.
- TERRACOL, M., SAGAUT, P. & BASDEVANT, C. 2001 A multilevel algorithm for large-eddy simulation of turbulent compressible flows. *J. Comp. Phys.* **167**, 439-474.
- WANG, B.-C., LEPOUDRE, P. P. & BERGSTROM, D. J. 2004 A direct solution method for the dynamic localization model for large-eddy simulation of turbulent flows with homogeneous dimensions. *Preprint*, submitted for publication.